

NUCLEAR DATA AND MEASUREMENTS SERIES

ANL/NDM-122

**Development and Testing of a Deuterium Gas Target Assembly for
Neutron Production via the $^2\text{H}(d,n)^3\text{He}$ Reaction
at a Low-Energy Accelerator Facility**

by

Dominique Feautrier and Donald L. Smith

March 1992

**ARGONNE NATIONAL LABORATORY,
ARGONNE, ILLINOIS 60439, U.S.A.**

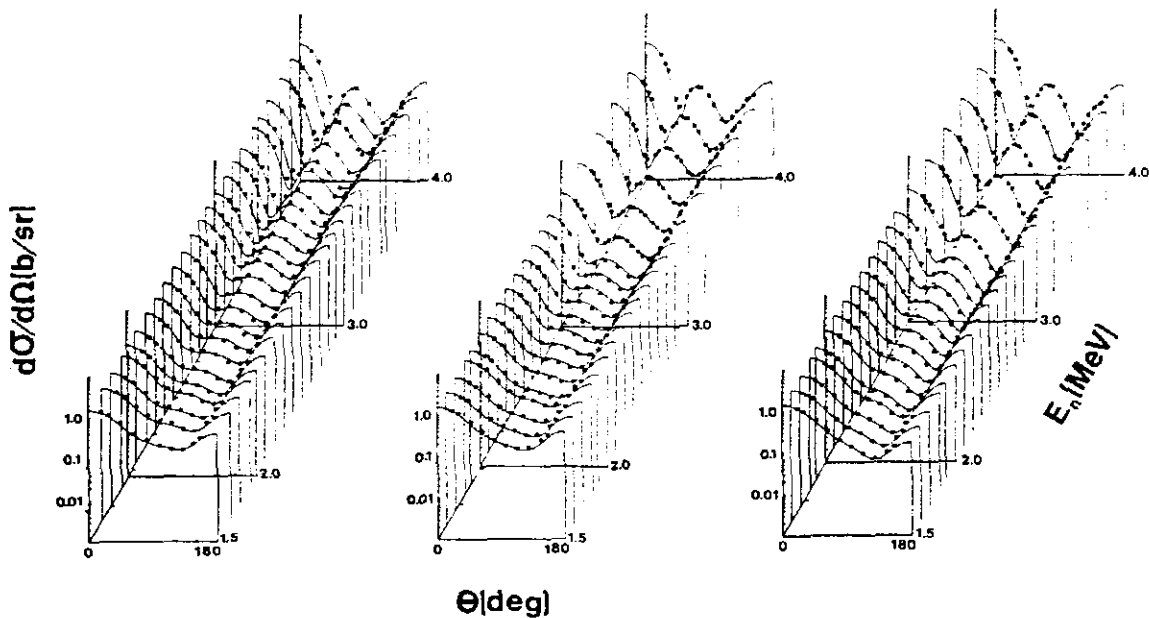
NUCLEAR DATA AND MEASUREMENTS SERIES

ANL/NDM-122

DEVELOPMENT AND TESTING OF A DEUTERIUM GAS TARGET
ASSEMBLY FOR NEUTRON PRODUCTION VIA THE $H-2(D,N)HE-3$
REACTION AT A LOW-ENERGY ACCELERATOR FACILITY

Dominique Feautrier and Donald L. Smith

March 1992



ARGONNE NATIONAL LABORATORY, ARGONNE, ILLINOIS

Operated by THE UNIVERSITY OF CHICAGO

for the U. S. DEPARTMENT OF ENERGY

under Contract W-31-109-Eng-38

Argonne National Laboratory, with facilities in the states of Illinois and Idaho, is owned by the United States government, and operated by The University of Chicago under the provisions of a contract with the Department of Energy.

DISCLAIMER

This report was prepared as an account of work sponsored by an agency of the United States Government. Neither the United States Government nor any agency thereof, nor any of their employees, makes any warranty, express or implied, or assumes any legal liability or responsibility for the accuracy, completeness, or usefulness of any information, apparatus, product, or process disclosed, or represents that its use would not infringe privately owned rights. Reference herein to any specific commercial product, process, or service by trade name, trademark, manufacturer, or otherwise, does not necessarily constitute or imply its endorsement, recommendation, or favoring by the United States Government or any agency thereof. The views and opinions of authors expressed herein do not necessarily state or reflect those of the United States Government or any agency thereof.

Reproduced from the best available copy.

Available to DOE and DOE contractors from the
Office of Scientific and Technical Information
P.O. Box 62
Oak Ridge, TN 37831
Prices available from (615) 576-8401

Available to the public from the
National Technical Information Service
U.S. Department of Commerce
5285 Port Royal Road
Springfield, VA 22161

**DEVELOPMENT AND TESTING OF A DEUTERIUM GAS TARGET ASSEMBLY
FOR NEUTRON PRODUCTION VIA THE H-2(D,N)HE-3 REACTION
AT A LOW-ENERGY ACCELERATOR FACILITY***

by

Dominique Feautrier** and Donald L. Smith

Engineering Physics Division
Argonne National Laboratory
9700 South Cass Avenue
Argonne, Illinois 60439
U.S.A.

March 1992

ACCELERATOR TARGET DEVELOPMENT. Deuterium gas target. H-2(d,n)He-3 reaction. Low-activation materials. Activation half lives. Activation cross sections. Neutron production. Low-neutron-background materials. High-current-capacity construction. Low-mass construction. Gridless target-window construction. Neutron background measurements. Residual activity measurements.

* This work was supported by the U.S. Department of Energy, Energy Research Programs, under contract W-31-109-Eng-38.
** Permanent address: Department Genie Mecanique, Ecole Normale Supérieure de Cachan, 61 Avenue du Président Wilson, 94235 Cachan, Cedex, France.

NUCLEAR DATA AND MEASUREMENTS SERIES

The Nuclear Data and Measurements Series presents results of studies in the field of microscopic nuclear data. The primary objective is the dissemination of information in the comprehensive form required for nuclear technology applications. This Series is devoted to: a) measured microscopic nuclear parameters, b) experimental techniques and facilities employed in measurements, c) the analysis, correlation and interpretation of nuclear data, and d) the evaluation of nuclear data. Contributions to this Series are reviewed to assure technical competence and, unless otherwise stated, the contents can be formally referenced. This Series does not supplant formal journal publication, but it does provide the more extensive information required for technological applications (e.g., tabulated numerical data) in a timely manner.

TABLE OF CONTENTS

	<u>Page</u>
INFORMATION ABOUT OTHER ISSUES OF THE ANL/NDM SERIES	5
ABSTRACT	9
1. INTRODUCTION	11
2. PHYSICAL PRINCIPLES OF THE DESIGN	14
3. ENGINEERING FEATURES OF THE DESIGN	19
4. PERFORMANCE TESTS	23
5. CONCLUSIONS	27
ACKNOWLEDGEMENTS	27
REFERENCES	28
TABLES	30
FIGURES	43

INFORMATION ABOUT OTHER ISSUES OF THE ANL/NDM SERIES

A list of titles and authors for all the previous issues appears in each report of the series. The list for reports ANL/NDM-1 through ANL/NDM-75 appears in ANL/NDM-76, and ANL/NDM-91 contains the list for reports ANL/NDM-76 through ANL/NDM-90. Below is the list for ANL/NDM-91 up to the current report. Requests for a complete list of titles or for copies of previous reports should be directed to:

Section Secretary
Applied Nuclear Physics Section
Engineering Physics Division
Building 314
Argonne National Laboratory
9700 South Cass Avenue
Argonne, Illinois 60439
U.S.A.

ANL/NDM-91 A.B. Smith, P.T. Guenther and R.D. Lawson, *On the Energy Dependence of the Optical Model of Neutron Scattering from Niobium*, May 1985.

ANL/NDM-92 Donald L. Smith, *Nuclear Data Uncertainties (Vol.-I): Basic Concepts of Probability*, December 1988.

ANL/NDM-93 D.L. Smith, J.W. Meadows and M.M. Bretscher, *Integral Cross-section Measurements for ${}^7\text{Li}(n,n't){}^4\text{He}$, ${}^{27}\text{Al}(n,p){}^{27}\text{Mg}$, ${}^{27}\text{Al}(n,\alpha){}^{24}\text{Na}$, ${}^{58}\text{Ni}(n,p){}^{58}\text{Co}$, and ${}^{60}\text{Ni}(n,p){}^{60}\text{Co}$ Relative to ${}^{238}\text{U}$ Neutron Fission in the Thick-target ${}^9\text{Be}(d,n){}^{10}\text{B}$ Spectrum at $E_d = 7$ MeV*, October 1985.

ANL/NDM-94 A.B. Smith, D.L. Smith, P. Rousset, R.D. Lawson and R.J. Howerton, *Evaluated Neutronic Data File for Yttrium*, January 1986.

ANL/NDM-95 Donald L. Smith and James W. Meadows, *A Facility for High-intensity Neutron Irradiations Using Thick-target Sources at the Argonne Fast-neutron Generator*, May 1986.

ANL/NDM-96 M. Sugimoto, A.B. Smith and P.T. Guenther, *Ratio of the Prompt-fission-neutron Spectrum of Plutonium-239 to that of Uranium-235*, September 1986.

ANL/NDM-97 J.W. Meadows, *The Fission Cross Sections of ${}^{230}\text{Th}$, ${}^{232}\text{Th}$, ${}^{233}\text{U}$, ${}^{234}\text{U}$, ${}^{236}\text{U}$, ${}^{238}\text{U}$, ${}^{237}\text{Np}$, ${}^{239}\text{Pu}$, and ${}^{242}\text{Pu}$ Relative ${}^{235}\text{U}$ at 14.74 MeV Neutron Energy*, December 1986.

ANL/NDM-98 J.W. Meadows, *The Fission Cross Section Ratios and Error Analysis for Ten Thorium, Uranium, Neptunium and Plutonium Isotopes at 14.74-MeV Neutron Energy*, March 1987.

ANL/NDM-99 Donald L. Smith, *Some Comments on the Effects of Long-range Correlations in Covariance Matrices for Nuclear Data*, March 1987.

ANL/NDM-100 A.B. Smith, P.T. Guenther and R.D. Lawson, *The Energy Dependence of the Optical-model Potential for Fast-neutron Scattering from Bismuth*, May 1987.

ANL/NDM-101 A.B. Smith, P.T. Guenther, J.F. Whalen and R.D. Lawson, *Cobalt: Fast Neutrons and Physical Models*, July 1987.

ANL/NDM-102 D.L. Smith, *Investigation of the Influence of the Neutron Spectrum in Determinations of Integral Neutron Cross-section Ratios*, November 1987.

ANL/NDM-103 A.B. Smith, P.T. Guenther and B. Micklich, *Spectrum of Neutrons Emitted From a Thick Beryllium Target Bombarded With 7-MeV Deuterons*, January 1988.

ANL/NDM-104 L.P. Geraldo and D.L. Smith, *Some Thoughts on Positive Definiteness in the Consideration of Nuclear Data Covariance Matrices*, January 1988.

ANL/NDM-105 A.B. Smith, D.L. Smith, P.T. Guenther, J.W. Meadows, R.D. Lawson, R.J. Howerton, and T. Djemil, *Neutronic Evaluated Nuclear-Data File for Vanadium*, May 1988.

ANL/NDM-106 A.B. Smith, P.T. Guenther, and R.D. Lawson, *Fast-neutron Elastic Scattering from Elemental Vanadium*, March 1988.

ANL/NDM-107 P. Guenther, R. Lawson, J. Meadows, M. Sugimoto, A. Smith, D. Smith, and R. Howerton, *An Evaluated Neutronic Data File for Elemental Cobalt*, August 1988.

ANL/NDM-108 M. Sugimoto, P.T. Guenther, J.E. Lynn, A.B. Smith, and J.F. Whalen, *Some Comments on the Interaction of Fast Neutrons with Beryllium*, November 1988.

ANL/NDM-109 P.T. Guenther, R.D. Lawson, J.W. Meadows, A.B. Smith, D.L. Smith, and M. Sugimoto, *An Evaluated Neutronic Data File for Bismuth*, November 1989.

ANL/NDM-110 D.L. Smith and L.P. Geraldo, *A Vector Model for Error Propagation*, March 1989.

ANL/NDM-111 J.E. Lynn, *Fifty Years of Nuclear Fission*, June 1989.

ANL/NDM-112 S. Chiba, P.T. Guenther, and A.B. Smith, *Some Remarks on the Neutron Elastic- and Inelastic-scattering Cross Sections of Palladium*, May 1989.

ANL/NDM-113 J.E. Lynn, *Resonance Effects in Neutron Scattering Lengths*, June 1989.

ANL/NDM-114 A.B. Smith, R.D. Lawson, and P.T. Guenther, *Ambiguities in the Elastic Scattering of 8-MeV Neutrons from Adjacent Nuclei*, October 1989.

ANL/NDM-115 A.B. Smith, S. Chiba, D.L. Smith, J.W. Meadows, P.T. Guenther, R.D. Lawson, and R.J. Howerton, *Evaluated Neutronic File for Indium*, January 1990.

ANL/NDM-116 S. Chiba, P.T. Guenther, R.D. Lawson, and A.B. Smith, *Neutron Scattering from Elemental Indium, the Optical Model, and the Bound-state Potential*, June 1990.

ANL/NDM-117 Donald L. Smith and Luiz P. Geraldo, *An Evaluation of the Nb-93(n,n')Nb-93m Dosimeter Reaction for ENDF/B-VI*, November 1990.

ANL/NDM-118 J.W. Meadows, *Characteristics of the Samples in the FNG Fission Deposit Collection*, December 1990.

ANL/NDM-119 S. Chiba, P.T. Guenther, A.B. Smith, M. Sugimoto and R.D. Lawson, *Fast-neutron Interaction with Elemental Zirconium, and the Dispersive Optical Model*, June 1991.

ANL/NDM-120 A.B. Smith, P.T. Guenther, J.F. Whalen, and S. Chiba, *Fast-neutron Total and Scattering Cross Sections of Ni-58 and Nuclear Models*, April 1991.

ANL/NDM-121 Satoshi Chiba and Donald L. Smith, *A Suggested Procedure for Resolving an Anomaly in Least-Squares Data Analysis Known as "Peelle's Pertinent Puzzle" and the General Implications for Nuclear Data Evaluations*", September 1991.

**DEVELOPMENT AND TESTING OF A DEUTERIUM GAS TARGET ASSEMBLY
FOR NEUTRON PRODUCTION VIA THE $H-2(d,n)He-3$ REACTION
AT A LOW-ENERGY ACCELERATOR FACILITY**

by

Dominique Feautrier and Donald L. Smith

ABSTRACT

This report describes the development and testing of a deuterium gas target intended for use at a low-energy accelerator facility to produce neutrons for basic research and various nuclear applications. The principle source reaction is $H-2(d,n)He-3$. It produces a nearly mono-energetic group of neutrons. However, a lower-energy continuum neutron spectrum is produced by the $H-2(d;n,p)H-2$ reaction and also by deuterons which strike various components in the target assembly. The present target is designed to achieve the following objectives: i) minimize unwanted background neutron production from the target assembly, ii) provide a relatively low level of residual long-term activity within the target components, iii) have the capacity to dissipate up to 150 watts of beam power with good target longevity, and iv) possess a relatively modest target mass in order to minimize neutron scattering from the target components. The basic physical principles that have to be considered in designing an accelerator target are discussed and the major engineering features of this particular target design are outlined. The results of initial performance tests on this target are documented and some conclusions concerning the viability of the target design are presented.

1. INTRODUCTION

Accelerators are used widely to produce a variety of neutron fields for nuclear basic research and technological applications [Cie83]. Fast neutrons in the several-MeV energy range can be generated easily at a small accelerator facility by means of the $H-2(d,n)He-3$ reaction [LP73,Utt83]. For example, at the Argonne National Laboratory Fast-neutron Generator (FNG) facility [CH71], incident monoenergetic deuteron beams in the energy range 2-7 MeV are used to generate nearly monoenergetic neutron fields with energies in the range 5-10 MeV [SM74] (the reaction is exoergic with $Q = 3.268$ MeV [MS80,Tul90]). This is a convenient neutron energy range for a number of nuclear-technology applications, and it is also a region of significant contemporary interest for cross-section studies relevant to both basic and applied concerns [Qai91]. In this domain, most of the neutron production associated with deuteron bombardment of deuterium indeed comes from the $H-2(d,n)He-3$ reaction, but for deuteron energies above 4.45 MeV, secondary neutron production is also observed from the $H-2(d;n,p)H-2$ reaction [Tul90]. These neutrons appear as a continuum contribution at lower energies in the spectrum. The relative yields and energy distributions of these "break-up" neutrons are reasonably well known so that corrections can be applied to measured data where required [SM74]. At higher energies (e.g., deuterons above 10 MeV), the break-up contribution increasingly dominates the total neutron production, but this is not the region of principal concern for the present investigation.

There are two distinct ways to make a deuterium target [Utt83]. The first involves a gas cell pressurized with molecular deuterium [e.g., HLS82, H0061, Ric60]. Collimated deuteron beams from the accelerator impinge upon the cell, entering through a window which is thin enough so that the deuteron-beam energy is not seriously degraded. At the same time, the window must be strong enough to contain the gas. The second approach utilizes a metal lattice with absorbed-deuterium gas. Titanium and zirconium are effective materials for this purpose [e.g., BS67,SCW67]. Although these particular metal-deuteride targets require special fabrication techniques, they can be obtained commercially. Such targets are physically relatively stable when not in use, but they do suffer from a number of operating deficiencies. One of these is the steady depletion of deuterium gas held in the lattice when bombarded with ion beams from an accelerator. This necessitates frequent replacement of the elements. Also, for a given level of neutron production, there is a relatively high energy loss in these targets for the primary deuteron beam, when compared to gas targets. This can lead to unacceptable broadening of the product-neutron energies. Although they have some unique limitations, gas targets are generally thought to be superior to metal-deuteride targets, so the latter were not considered. Details on various earlier deuterium-target designs appear in the literature [Gin+76,HLS82,Hoo61,Jon+57,OT86,Ric60,Woj+88]. The present study deals only with the design and testing of

a particular gas-target assembly developed for use at the FNG facility. Two other designs have been employed previously at this facility. One of these was developed for high-current applications, e.g., the measurement of neutron-activation cross sections. It employs a relatively-massive gridded assembly to support the gas-target window. The other design incorporates a self-supporting window and has a very low mass to minimize neutron scattering perturbations. It has a limited deuteron-beam current capacity which, however, is consistent with its normal use with pulsed and bunched beams for time-of-flight measurements. The present target design aims to merge certain properties of these earlier designs, and to incorporate some new features which were previously not addressed. In particular, this target aims to satisfy these design objectives:

1) Relatively high-current capacity---

The target is intended primarily for use in neutron-activation cross section studies and for applied neutron irradiations where relatively high neutron fluences are desirable. The FNG accelerator can routinely produce 20+ microampere beams of ≥ 7 -MeV deuterons, corresponding to a beam power of ≤ 150 watts. Therefore, it is intended that the target be able to survive for a reasonable time period (at least 24 hours of intermittent use) under these operating conditions.

2) Low-activation materials---

This feature is particularly important in striving to meet contemporary environmental, safety and health (ES&H) standards for the operation of nuclear facilities, and for implementing ALARA (As Low as Reasonably Achievable) principles for personnel radiation exposures. To achieve this objective involves the minimal use of materials which can be transmuted by the incident radiations (deuterons and neutrons) to produce relatively-long-half-life reaction products.

3) Minimal perturbation of the primary neutron spectrum---

The $H-2(d,n)He-3$ reaction is normally used in applications where monoenergetic neutrons are desired. Therefore, it is required that the usable neutron field be perturbed as little as possible through neutron absorption and scattering interactions within the target.

4) Low neutron background---

Target components which are bombarded with the primary and scattered deuterons must be chosen for minimal background neutron production. All other target components must then be shielded adequately from energetic deuterons.

5) Modular construction---

The target engineering design itself must provide for easy assembly and disassembly of the unit as well as for convenient handling of those components which must be replaced relatively

frequently (e.g., the target window foils). Also, those components which are more prone to become radioactive during use should be readily separable from the rest of the unit to facilitate storage of the target assembly when it is not in use.

Section 2 of this report discusses certain basic physical principles relevant to the development of the target. The thermal, mechanical and nuclear properties for a number of materials were considered in selecting a particular design. Figures of merit based on various pertinent physical parameters have been devised to provide a quantitative basis for these comparisons. Section 3 discusses the chosen engineering design for the target assembly. Finally, the results of performance tests on the actual unit are reported in Section 4. The conclusions of this study are summarized in Section 5.

2. PHYSICAL PRINCIPLES OF THE DESIGN

Each of the five design objectives discussed in Section 1 demands consideration of certain fundamental physical principles. We shall now examine these areas in some detail. For a variety of practical reasons, we restrict our consideration of target materials to the following pure elements (and compounds or alloys formed from these elements): aluminum (Al), carbon (C), chromium (Cr), cobalt (Co), copper (Cu), fluorine (F), gold (Au), iron (Fe), molybdenum (Mo), nickel (Ni), platinum (Pt), tantalum (Ta), titanium (Ti), tungsten (W), and vanadium (V). The various isotopes of these elements are listed in Table 1 along with their natural abundances [Tul90].

Adequate cooling of the target assembly is an important engineering requirement which must be addressed in any target design considered. (Item 1 from Section 1). In order to be able to dissipate up to 150 watts of beam power, the target assembly must be quite sturdy. Those components which are exposed to the greatest heat load, or are in direct contact with such components, must be constructed from materials which possess reasonably good thermal conductivities and/or relatively high melting points. The latter requirement is especially important in the case of those components which can experience the brunt of the focused deuteron beam, very possibly concentrated in a "hot spot" $\leq 0.2 \text{ cm}^2$ with a potential power density $\geq 750 \text{ watts/cm}^2$. Elevated temperatures can be expected at these locations. Table 2 lists the melting points and thermal conductivities of those materials which have been considered in developing this target assembly [Wea86]. These parameters were given very careful consideration in the selection of materials for fabricating the critical components. However, since other constraints are involved in the target design (e.g., availability and cost), the materials with the highest melting points and thermal conductivities are not necessarily the ones which were selected for a particular application. Experience in this laboratory has shown that gas targets operating at normal beam-current levels must be cooled explicitly by some active means. That is, there must be a mechanism for transporting heat out of the target other than passive conduction, convection or thermal radiation. The target design of Guenther [Gue91] relies entirely on an external air jet for this purpose while the gridded target design of Meadows et al. [MSW80] employs both water cooling and an external air jet. In the present design both an external air-jet and water cooling are employed, as is discussed in more detail in Section 3.

An important objective of the present target design concerns minimization of residual target radioactivity (Item 2 from Section 1.) Components exposed directly to incident deuterons from the accelerator (or possibly to scattered deuterons) can be transmuted by nuclear reactions, in particular via the (d,n) and (d,p) processes. Neutrons, which are far more penetrating than deuterons and, therefore, impinge upon all parts of the target assembly can also induce radioactivity by (n,n'), (n,p), (n, α), (n,d), (n;n,p) and (n,2n) reactions. These

various processes will leave the afflicted target components radioactive unless the product nuclei are stable. The presence of these residual activities can introduce problems related to the handling, storage and eventual disposal of used target-assembly components. If the target is very radioactive after a long run, anyone who is required to work near the target, e.g., to replace a damaged entrance-window foil or to remove the entire target from the beam line (and possibly disassemble it) during the course of an experiment, will be exposed to radiation. It is desirable to minimize this exposure in accordance with ALARA principles, as indicated in Section 1. Consequently, it is important to seek materials with activation "vulnerabilities" that are as low as possible. If unavoidable activities are produced, they ought to be relatively short-lived so that the target can be handled safely after a modest waiting time. Eventually, it is necessary to either store the target for long periods between experiments or to dispose permanently of certain "used" components. Then, the level of long-term activity accumulated in the target by normal use should be as low as possible. This particular requirement also points toward the use of materials that transmute to either stable or short-lived products.

A number of physical factors conspire to influence the relative importance of those activation processes which must be considered. Among these are the reaction Q -values or, equivalently (where applicable) the corresponding thresholds, the half lives of the reaction-product nuclei, the nature of the induced radioactivity, and the reaction cross sections. With the exception of cross sections, these requisite parameters are readily available from compilations to be found in the literature [Tul90,LS78]. Some knowledge of the reaction cross sections is important in making these assessments but this is a relatively complex matter as we shall see below. Neutron cross-section estimates are generally readily available, e.g., in this investigation we referred to BNL-325, a published compilation of cross-section plots by McLane et al. [MDR88], in order to obtain reasonable values for these parameters. In principle, knowledge of the neutron cross sections at all energies up to the maximum encountered is required. For convenience, we have only tabulated the cross-section values for 10-MeV neutrons (the probable upper end of the energy range for applications of this target in our laboratory). This is a useful energy for comparison purposes because many of the threshold reaction processes considered attain maximum cross-section values in this region. Cross sections for deuteron-induced reaction processes are, at best, difficult to come by and, in most instances, are simply not available. Again, knowledge of these cross sections would be required at all deuteron energies from zero (or threshold if the reaction Q -value is negative) up to the maximum available incident energy from the accelerator. We decided to avoid this problem by omitting direct consideration of deuteron-reaction cross sections in our analysis. Subjective judgments involving these cross sections can be made by noting that larger positive Q values (as indicated above) and lower atomic numbers (Z) generally lead to relatively greater deuteron-induced-reaction cross sections. The parameters which we assembled explicitly for the present analysis are compiled in Tables 3-8.

In order to provide a moderately-objective basis for quantitative comparison of the activation vulnerability of various materials, we have defined a composite activation-vulnerability parameter, V_A , which combines those parameters described above in a physically meaningful fashion. The formula we have employed for this purpose is

$$V_A(t) = \sum_{i,j} (1/\tau_{ij}) \cdot n_i \cdot \sigma_{ij} \cdot \exp(-t/\tau_{ij}), \quad (1)$$

where the index "i" designates a particular isotope present in the material, "j" indicates a particular reaction process, n_i represents relative isotopic density, σ_{ij} is the reaction cross section (in millibarn) and τ_{ij} is the mean life time of the reaction product (i.e., the half life divided by $\ln 2$). In applying this formula, we have chosen to express τ in terms of days to provide a consistent normalization standard for the calculation of V_A . V_A is clearly time dependent, i.e., relative material-activation vulnerability changes according to the time, t , which has transpired following the irradiation. In this context, comparisons have been made for $t = 1$ hour (0.04167 day), 1 day, 1 week (7 days), 1 month (30 days) and 1 year (365 days). The significance of these selected times is as follows: One hour is a typical time frame for approaching the target area at the end of a run to remove samples, adjust equipment, possibly replace damaged target-window foils, etc. One day (or overnight or over a weekend) is typical of waiting times between distinct portions of an experiment, or before performing major adjustments to an experimental setup. One week to one month is the typical time frame during which one might allow the target activity to die away sufficiently to remove the unit from the beam line for storage or for complete disassembly of the components. Finally, one year is a convenient time frame for judging the long-term activity build-up vulnerability of target materials from the point of view of waste disposal.

Tables 9-10 present the results of calculations for V_A upon which to compare the activation vulnerabilities of various materials considered in this study. In principle, these calculations should be carried out using realistic values for σ_{ij} , the various relevant deuteron-induced, activation-reaction cross sections. Such information is difficult to obtain and often is very speculative. Consequently, no such information was compiled in this work, and $\sigma_{ij} = 1$ was assumed throughout in calculations of V_A for Table 10. Since these values of V_A do not reflect realistic cross section values, they cannot be compared directly with those associated with neutron-induced reactions (Table 9). In fact, they can be examined only on a qualitative basis with respect to other deuteron-induced reaction processes.

The next issue of physical concern from Section 1 is Item 3, namely, perturbation of the primary neutron spectrum. It is desired to minimize this effect. What is involved here is the scattering of primary neutrons (emitted from the source) by components of the assembly. Generally speaking, the more physically-massive the assembly, the greater the scattering perturbation. Scattering

perturbations can be reduced by paring the size of the assembly components to the bare minimum, consistent with other requirements of the design such as cooling. However, matters are not quite so simple when one examines the details. The extent to which various parts of the gas target contribute to the scattering also depends upon the specific materials and scattering processes involved, the distances of the scatterers from the source volume, their geometric positions in relation to zero degrees (i.e., the incident beam direction), and the intended irradiation position. If the more-massive portions of the target assembly are situated as far as possible from the source volume, this will minimize the scattering perturbations for those irradiations that take place fairly close to the target (e.g., irradiations for most neutron-activation or neutron-fission studies). However, if the irradiation position for an experiment is located far from the target relative to the dimensions of the target assembly, then this point is rather irrelevant. However, if the more massive portions of the target assembly are situated toward back angles (> 90 degrees relative to the incident beam line), while the intended position of irradiation for the experiment is in the forward direction, then the scattering perturbations also will be considerably reduced. Neutron-scattering distributions tend to be rather strongly forward-peaked, especially for the dominant elastic scattering process at higher neutron energies. In the case of scattering from hydrogen, back-angle scattering is actually excluded by kinematic considerations. Most gas-target designs, including the present one, strive to exploit this particular physical phenomenon. We have defined a scattering-vulnerability parameter, V_s , which can be calculated for each material considered for the design. For simplicity, we have chosen the integrated macroscopic integrated elastic scattering cross section at 10 MeV as the parameter for comparison (even though this over-simplifies the situation considerably). The formula is

$$V_s = \sum_i n_i \cdot \sigma_{el,i}, \quad (2)$$

where the index "i" designates the particular isotope or element present in the material, n_i is the atomic density for that isotope or element (atoms/cm³) and $\sigma_{el,i}$ is the corresponding integrated elastic-scattering cross section. We have obtained values of $\sigma_{el,i}$ from McLane et al. [MDR88]. Note that this vulnerability parameter does not take scattering angular distributions or inelastic scattering into consideration, and that only one neutron energy, namely, 10 MeV, is considered. The results of our scattering-vulnerability analysis, based on Eq. (2), appear in Table 11.

Finally, we address the issue labelled Item 4 in Section 1, namely, background-neutron production from the gas-target cell. In some experiments, e.g., neutron activation studies, the effects of background neutrons can be (and indeed should be) measured directly. Nevertheless, it is desirable to keep such perturbations at a minimum. Basically, neutrons are produced by (d,n) reactions wherever the direct beam strikes the target. There is also a slight possibility that elastically scattered deuterons can produce observable neutrons

when they impinge upon target surfaces which normally do not see the direct beam. Experience in our laboratory has shown that the best way to minimize this effect is to insure that the deuterons are permitted to strike only surfaces of materials with high atomic numbers (Z). In the present design we have limited our consideration to gold (Au), tantalum (Ta), tungsten (W). However, in our laboratory there is one light element which cannot be avoided completely, namely, carbon (C). The reason is that hydrocarbon materials (from the oil-vapor diffusion pumps which are used to produce the vacuums on the accelerator beam lines of our facility) inevitably build up on target surfaces. The quantities of material involved are usually very modest, and the effect can be minimized by frequently cleaning or replacing those components with critical surfaces. For the reasons mentioned above, we have not attempted to calculate the background neutron yields for these materials. Instead, we have undertaken to measure the relative neutron production from several possible beam-stop materials, in a separate experiment using a flat-response neutron detector. This investigation is discussed in detail in Section 4.

3. ENGINEERING FEATURES OF THE DESIGN

The main difference between the present target design and the earlier high-current design from this laboratory [MSW80] is the absence of a window-foil support grid. We shall now examine the reason why we sought to eliminate this grid from the design. It is true that a grid provides a sturdy support for the target-window foil as well as an additional mechanism for dissipating heat deposited in the window through ionization energy loss of the beam. However, there are serious disadvantages. One is that such grids are difficult and expensive to fabricate, and are hard to maintain in normal usage. The grids must be polished each time a window is replaced. Even then, they tend to develop sharp edges and burrs which can easily puncture the window foil when the cell is placed under pressure. Furthermore, the grids become dirty and eventually are observed to produce unacceptable background neutron yields. Troublesome carbon buildup from the disassociation of hydrocarbon compounds in the vacuum system (see Section 2) and stray epoxy residues are difficult to remove from grid surfaces without damaging their fragile structures. We have found that the only way to do this effectively is to play the flame from an oxygen-acetylene torch directly across the grid surface. This must be done very carefully to avoid melting the grids, which are expensive to replace. Such problems are avoided completely by resorting to a gridless target design.

The present gas-target assembly is shown schematically in Figs. 1 and 2. Photographs of several key components appear in Figs. 3-5, and Figs. 6 and 7 present photographs of the assembled unit. In this section we will examine each aspect of the design. It is suggested that the reader refer to these figures, as well as to Tables 1-11 during the course of the following discussion.

The beam stop at the end of the target cell (component "b" on Fig. 1) must be thick enough to stop the beam and, also, it must offer sufficient rigidity to maintain the integrity of either a vacuum or deuterium gas under about 2 atmospheres of pressure, as the case may be. We have learned, from our experience with gridded cells [MSW80], that thicknesses of at least 0.020 inch (0.05 cm) are needed to meet these requirements for the conditions in our laboratory. However, it is also important to minimize neutron scattering and absorption perturbations by keeping the beam stop as thin as possible. In the present design, we incorporate beam stops which are nominally 0.020-0.030 inch thick, as a compromise between these conflicting requirements. Deuterium gas from the incident beam (i.e., from "drive-in" deuterons) eventually builds up in the beam stop. Since this leads to structural weakening (radiation damage) as well as to an increase in background neutron yield, beam stops must be replaced rather frequently in normal use. Several factors need to be considered in choosing the material for the beam stop. In most physical respects, gold is ideal. The induced activities from (d,n) and (d,p) reactions have relatively short half lives (Tables 3 and 4) leading to a low calculated radiation vulnerability for gold

(Table 10). Also, the thermal conductivity of gold is very good and its melting point is high enough to sustain typical thermal loads from the beam, as long as external cooling is provided. The main problem with gold is its high cost, which is prohibitive for most applications. We have not considered platinum for use in the present design because there are activities with longer half lives involved and, usually, even higher costs to bear in acquiring this material than for gold. For these reasons, we chose to limit our consideration of practical beam stop materials to tantalum and tungsten. Both of these have very high melting points (Table 2). The thermal conductivity of tungsten is superior to tantalum (Table 2), but tantalum is easier to machine. The short-term radiation vulnerability of tungsten is larger than for tantalum. Over the long term, tungsten is superior in this category, but both tantalum and tungsten appear to provide tolerable levels of long-term radiation vulnerability (Table 10). Ultimately, we selected tantalum for the present design because of its superior mechanical properties and ease of machining. Since beam stops are easily interchanged, other materials could be tested and employed in the future if this proves to be advantageous. The beam stop is clamped into position (component "a" in Fig. 1) to insure that it is kept firmly seated against the O-ring seal on the gas cell under all operating conditions.

The gas cell itself (component "c" in Fig. 1) has a relatively low mass to minimize neutron scattering effects near the source volume (i.e., the region where the incident deuteron-beam intercepts the deuterium filler gas in the cell). A number of materials were considered for the construction of this cell. The important considerations were: good thermal conductivity, structural integrity, low radiation vulnerability and convenience of fabrication. In the final analysis, the choice was narrowed to stainless steel, aluminum and copper. Since it was evident qualitatively that some of the neutron-induced activities in iron and other prominent constituents of stainless steel (nickel, chromium, etc.) would lead to unfavorable long-term neutron vulnerabilities, it was eliminated from consideration without performing any detailed vulnerability calculations. Aluminum is the optimal material from the point of view of long-term radiation vulnerability, but from the thermal and mechanical points of view, it is inferior to copper. These latter considerations are important because the gas cell is quite small and must dissipate considerable heat during normal operation. In this context, copper was the only material to which a cooling tube (component "l" on Fig. 1) could be attached easily by soldering. Therefore, copper was selected as the best all-around material for fabricating the main body of the gas cell. Two tubes (component "m" on Fig. 1) are attached to the body of the cell (on opposite sides). These provide for evacuation of the cell and its pressurization with deuterium gas. Each tube has an integral fitting which permits external tubing to be attached, thereby connecting the cell with either the vacuum system or a deuterium gas supply.

The gas cell is mounted to a flange (component "f" in Fig. 1) which also holds the secondary deuteron beam aperture (component "e" in Fig. 1). Aluminum is clearly the best choice for this component

for the reasons mentioned above. Also, the macroscopic elastic-scattering cross section for aluminum is much lower than that for copper, the alternative possibility, thereby leading to reduced neutron-scattering perturbations to the primary source from this relatively-massive component of the target assembly. For the same reasons, aluminum was chosen for another flange (component "h" in Fig. 1), which serves to hold the primary aperture (component "i" in Fig. 1).

The primary aperture bears the main responsibility for defining the deuteron beam which enters the cell. It is smaller than the secondary aperture, so very few, if any, of the incident deuterons transmitted into the cell will strike the edge of the secondary aperture. The secondary aperture is spanned by a self-supporting target-window foil (component "o" in Fig. 1) which is held in place and vacuum-sealed by epoxy. The edge of this aperture is well-rounded and polished in order to provide a smooth, burr-free support surface for the window foil. The secondary aperture plate is clamped firmly to its aluminum support flange by a tantalum ring (component "d" in Fig. 1) to insure that the O-ring seals tightly to hold either a good vacuum or maintain the deuterium gas under pressure. The primary and secondary apertures are fabricated from tantalum for the same reasons discussed above, in connection with the beam stop.

Although it is not shown in Fig. 1, exposed surfaces of those target assembly components which are fabricated from materials with lower atomic numbers can be shielded with thin (< 0.010 -inch) tantalum foil to avoid possible interactions of secondary deuterons that are scattered from aperture plates. This precaution may be taken to reduce the unwanted background neutrons from the cell and minimize production of any additional residual activities.

Both nickel and molybdenum have been used previously for fabricating target cell windows [MSW80,Gue91]. Overall, we have had the best success with molybdenum, so it was selected without reservations for the present design. The window thicknesses are typically in the range 2-6 mg/cm². The foils are carefully weighed and the foil areas are measured as a means to ascertain the foil thicknesses. Deuteron bombardment of molybdenum produces residual activities. We have calculated corresponding radiation vulnerabilities for molybdenum so that they can be compared qualitatively with those for the beam stop materials (Table 10). However, it should be kept in mind that variations in cross section, deuteron-beam energy, and geometry will lead to considerable differences between the residual radiation levels found in the beam stop, the aperture plates and the gas-target-window foil. The same can be said for background neutron production. Both of these issues can be explored best by experimental observations.

Cooling is an important consideration of the present design. As with the previous target designs from this laboratory [MSW80,Gue91], an external air jet is directed against the target cell to aid in its cooling. Furthermore, water cooling is used, as in the gridded target design of Meadows et al. [MSW80]. Unlike the earlier design, water

cooling is also provided directly to the target cell, close to the beam-stop O-ring groove to insure preservation of a critical O-ring seal (component "l" on Fig. 1 or "a" on Fig. 2). The approach is similar to that described by Gindler et al. [Gin+76]. Both aluminum aperture flanges (components "f" and "h" on Fig. 1 or "d" on Fig. 2) are cooled by means of internal water-cooling channels located symmetrically on three sides of each unit (component "c" on Fig. 2). All of these cooling tubes and channels are connected in series to a chilled water source, to insure positive flow through the entire target assembly.

The present target design incorporates two electrical insulating flanges (components "g" and "j" on Fig. 1). These isolate both the target assembly and the primary aperture assembly so that beam current can be measured independently from both entities, if required, and, also, so biases can be applied to suppress secondary electron emission which might interfere with the precise measurement of beam currents. These insulators could be fabricated from teflon, nylon, lucite or other suitable insulating materials which can be machined readily. Lucite was chosen for the present design because it was conveniently available in the machine shop.

It is evident from Fig. 1 that most of the target mass is situated at back angles relative to the beam line intercept with the gas cell. Since the primary neutron yield from the $H-2(d,n)He-3$ reaction is forward peaked, the present design tends to minimize scattering perturbations to the neutron field in the forward direction where most experiments are performed. This was also the case in the design of Meadows et al. [MSW80].

The various target components are held together by machine screws. Viton-A O-rings, as indicated in Fig. 1, are used to maintain the required vacuum and pressure seals. The entire assembly is attached to a flange (component "p") on the FNG accelerator beam line by means of nylon screws, to maintain integrity of the electrical insulation. Each piece is aligned to fit together with neighboring members by means of centering shoulders and recesses which are machined, either undersized or oversized, as needed to allow for loose fitting at room temperature, and to provide some leeway for expansion at higher operating temperatures.

4. PERFORMANCE TESTS

All of the experimental tests that were carried out on the present target, as described below, involved use of 5-MeV deuteron beams from the Argonne FNG accelerator [CH71]. The deuteron-beam energy was determined by magnetic analysis, and the current was measured using a beam-current integrator [CH71]. A 1-Megaohm resistor was installed to ground from the target, in parallel to the current integrator lead (which has an input impedance of less than 10 Ohm). This resistor provided insurance against buildup of charge on the target in the event that the target-current lead to the current integrator were to become detached accidentally during the measurements. At the same time, the 1-Megaohm resistor offered a negligible perturbation to the charge-recording circuitry. The beam-defining aperture plate was grounded to prevent any buildup of charge on this component as well. If required, this aperture could be biased to suppress secondary-emission electrons from the target. However, this was not done during these tests. Since the circulating cooling water was somewhat ionized, leakage of current to ground was observed during test operation of the target assembly. This usually amounted to ≤ 0.1 microamperes, which was relatively insignificant compared to the operating deuteron-beam currents of 2 or more microamperes which were normally encountered during the tests of this unit.

Before any target tests were performed in-situ at the FNG accelerator facility, the entire target assembly was bench-tested for vacuum leaks using a helium leak checker. No such leaks were found, so the complete unit (minus the molybdenum-foil window) was assembled on a selected beam line at the FNG. Again, no vacuum leaks were observed for the unit in place. Water-cooling tubes were then attached, and water was circulated through the components in series in accordance with the design plan. The flow rate for this setup was found to be about 20 liters per hour. A simple calculation showed that the rise in the cooling-water temperature that could be expected at this flow rate would be less than 5 degrees Centigrade for a beam power of 100 watt (e.g., corresponding to 20 microampere of deuteron beam current at 5-MeV energy). This is a tolerable rise in the temperature which, actually, is quite beneficial since it tends to alleviate potential problems due to the condensation of atmospheric moisture on the surface of the target assembly during warm, humid days. However, if a larger water-flow rate were to be required, this could be achieved easily by increasing the diameters of the water-cooling lines attached to the target, and of the cooling channels inherent to the target components themselves.

For the beam-on tests, the target assembly was situated in a well-shielded enclosure which has been described previously [SM86]. This particular FNG station offers a collimated port in the zero-degree direction which enables the neutrons emitted in the forward direction to be monitored by a detector placed outside the shielded enclosure. A BF_3 long counter was used for this purpose in

the present investigation. This detector provides a relatively-flat efficiency response to neutrons over a fairly-wide energy range (tens of keV to several MeV) and, therefore, was suitable for qualitative measurements of fast-neutron yields from the target.

The first tests with deutron beams on the target were performed without the presence of a molybdenum-foil window. The purpose was to compare the relative production of background neutrons from various target beam-stop materials. The materials tested were, in order of ascending atomic number, carbon ($Z = 6$), molybdenum ($Z = 42$), tantalum ($Z = 73$), tungsten ($Z = 74$), platinum ($Z = 78$), and gold ($Z = 79$). Each beam stop used was thick enough to stop the incident 5-MeV deuterons. Naturally, carbon would be a very poor choice for a beam stop material, but the present measurements with carbon were merely intended to provide an estimate of the maximum background-neutron contamination that could be expected from potential carbon buildup in the target during use. Molybdenum is also an unfavorable choice for a beam stop material but, during normal operation, the deuterons must pass through a molybdenum window foil in the gas cell, so some neutron production from (d,n) reactions on molybdenum is unavoidable. The present measurements with a molybdenum beam stop provide an indication of the relative importance of background-neutron production from deuterons incident on molybdenum. The beam-stop measurements consisted of recording the long-counter and current-integrator readings for runs taken with each of the examined beam-stop materials. The ratio of long-counter counts to integrated current provided an adequate measure of the relative neutron yield from each beam stop used. Since the absolute yield scale is unimportant, we have chosen to present the results using a relative scale, in which the material tantalum is arbitrarily given the value of unity (i.e., "1"). On this scale, the results of the present tests are as follows: carbon (558.1), molybdenum (3.96), tantalum (1.000), tungsten (1.36), platinum (0.508), and gold (1.05). These results are rather qualitative because the observed yield from each beam stop depended not only on the predominant material of the beam stop but also on impurities present, and on any local surface contamination. Nevertheless, these results are entirely consistent with what would be expected on the basis of the discussion in Section 2. Clearly, tantalum, which is the chosen beam-stop material for the present design, is quite acceptable as a relatively modest producer of background neutrons.

Next, the tantalum aperture plate, with a 3.28 mg/cm^2 molybdenum foil attached to it and sealed against pressure leaks by epoxy, was installed in the gas-target unit which was situated on the beam line. No vacuum leaks were observed. The cell was charged with deuterium gas at 2 atmospheres pressure (≥ 28 psi absolute). Afterwards, the cell was pumped to a vacuum and subsequently recharged with deuterium to 2 atmospheres pressure, in order to purge the system of any contaminant gases. No leaks were observed at this pressure. A deutron beam of relatively low intensity (≤ 2 microamperes) was then directed into the gas cell. The incident beam was swept very slightly in both the horizontal and vertical directions at 60 Hz using air-core magnetic-sweep coils. The purpose was to avoid formation of a beam

hot spot that could puncture the molybdenum-foil window. No leaks or other evidence of target deterioration were observed under these conditions, so the beam current was gradually increased to 15 microamperes. The neutron-production rate was monitored using the long counter with an attached ratemeter. The neutron yield was observed to remain essentially proportional to the incident current up to about 10 microamperes. At higher beam currents, some decrease in the neutron production rate was observed, presumably due to the target-heating effect described previously by Meadows et al. [MSW80]. In fact, the gas pressure in the target was observed to have increased by about 1 psi by the time the incident beam current had been raised to 15 microamperes. A steady beam was maintained on the target at the 15-microampere level for about an hour. No signs of target deterioration were observed. The beam current was then reduced to zero at a gradual rate, but much more quickly than it was raised. The target was evacuated and refilled a couple of times to test the effect of varying pressure conditions on the target after having survived the irradiation conditions described above. Deuterium gas-in (at 2 atmospheres pressure) and empty-cell measurements were then made with about 3 microamperes of current on target to determine the relative numbers of background -and primary-reaction neutrons from the target. Based on the long-counter data, it was found that <5% of the neutron yield could be attributed to background. Note that this included neutrons from the molybdenum-foil window. The beam was again directed onto the target. This time, it was raised steadily to 20 microamperes over a time interval of about 15 minutes. The beam was maintained on target for about 10 minutes near this level (which occasionally reached as much as 21 microamperes). Under these conditions, it was determined that the total power dissipated in the target was at the rate of about 100 watts. Of this total beam power, ~ 4 watts were expended in the molybdenum-foil window, ~ 3 watts were dissipated in passing through the deuterium gas itself and the remainder, ~ 93 watts, were deposited in the tantalum beam stop. At the end of these runs, it was observed that the molybdenum foil had sustained no visible damage (certainly it did not leak). In fact, the molybdenum foil actually looked better after it was used than before (the metal had a shinier finish)! The side of the tantalum beam stop which formed an inner wall of the gas cell was not noticeably affected. However, the exterior of the beam stop (which was in contact with air) was visibly affected. There was an accumulation of white powder in the vicinity of the beam axis, which we speculate was tantalum oxide formed by the oxidation of hot tantalum metal in the presence of atmospheric oxygen. This beam stop was 0.05-cm thick. Clearly, it would not have survived much longer under the conditions of these tests, so we conclude that a thicker beam stop should be used for this target, perhaps ~ 0.1-cm thick, whenever beam currents exceeding 10 microamperes are employed. With this proviso, we conclude that the target is capable of satisfying the design goals, and meets all the practical requirements of a high-current target to be used for neutron-irradiation experiments at an accelerator facility comparable to the PNG.

Following the target tests with deuteron beams, as described above, some qualitative measurements were made of residual target

radioactivity. The target was approached with a beta-gamma survey meter about 5 minutes after the beam was removed from the target. Due to the position of the target in the irradiation cavity [SM86], it was not possible to place the survey meter any closer than about 15 cm from the target (at a back angle). In this configuration, the activity measurements were mainly sensitive to gamma rays. Initially, the measured activity was about 6 mR/hour (a quite modest level). The activity was then remeasured at several intervals over a period of 20 hours following the initial measurement, leading to the following results (expressed as a percent of the initial 6 mR/hour activity): 0.3 hour (60%), 1.1 hour (30%), 3.0 hours (17%), and 20 hours (< 2%). So, the initial external activity of the target is relatively low and it drops off to a negligible level after about a day. Consequently, we are quite justified in considering this a low-activation unit. When the target was disassembled, it was observed that the radioactivity levels were very modest indeed (even for beta particles) for all the components except the molybdenum foil. This foil was observed to be quite radioactive on the day following the irradiation (over 100 mR/hour in contact with the foil, due mainly to beta activity of various technetium isotopes). The remaining components of the target present no serious hazards for handling and storage at modest times following its use. Since the predominant activity of the target assembly is indeed confined to a very small metal foil (which can be safely stored or disposed of under the control of radioactive-waste-management personnel), it is found that this target assembly is very convenient to use in the laboratory environment.

5. CONCLUSIONS

This cell was found to perform exceptionally well up to the design objective of 20 microamperes. Although it was tested with a deuteron-beam energy of 5 MeV rather than 7 MeV (corresponding to 100 watts of beam power rather than closer to the design maximum of ~ 150 watts), it is anticipated that the target will be able to operate successfully at the higher-power level because the present tests resulted in no visible signs of damage to the molybdenum foil (which is potentially the unit's most vulnerable component). The gridless design this target incorporates results in lower empty-cell (no deuterium filler gas) neutron backgrounds than the earlier target design of Meadows et al. [MSW80] which utilizes a grid. It also offers a higher primary-neutron yield potential than the gridless cell (for a given beam energy and current) because there is no grid present to obstruct the beam. The residual radioactivity of the target assembly on the day following the test measurements was found to be confined almost entirely to the molybdenum-foil window. If desired, this problem could be mitigated by using a different window material (e.g., gold). Consequently, storage of the unused target assembly appears to pose no significant problems. Finally, the present design makes it much easier to regenerate the target (install a new foil window) than the gridded design because there is no need to be concerned over the possibility of damaging delicate grid structures during the cleanup process.

ACKNOWLEDGEMENTS

The authors are indebted to J. Fabish, P.T. Guenther, J.W. Meadows and A.B. Smith from this laboratory for their contributions to this work. V. Davis assisted in laying out the figures of this report. Discussions with P. Ryge and Z.P. Sawa of Science Applications International Corporation, Santa Clara, California are also gratefully acknowledged.

REFERENCES

- BS67 K.G. Broadhead and D.E. Shanks, Int. J. Appl. Radiat. Isot. 18, 279 (1967).
- CH71 S.A. Cox and P.R. Hanley, IEEE Trans. Nucl. Sci. NS-18, 108 (1971).
- Cie83 S. Cierjacks, "Introduction", Neutron Sources for Basic Physics and Applications, ed. S. Cierjacks, Pergamon Press, Oxford, U.K. (1983).
- Gin+76 J.E. Gindler, M.C. Oselka, A.M. Friedman, L.W. Mayron and E. Kaplan, Int. J. Appl. Radiat. Isot. 27, 330 (1976).
- Gue91 P.T. Guenther, Argonne National Laboratory, private communication (1991).
- HLS82 S.-J. Heselius, P. Lindblom and O. Solin, Int. J. Appl. Radiat. Isot. 33, 653 (1982).
- Hoo61 A.M. Hoogenboom, Rev. of Sci. Instr. 32, 1395 (1961).
- Jon+57 K.W. Jones et al., Rev. Sci. Instr. 28, 1, 57 (1957).
- LP73 H. Liskien and A. Paulsen, Nuclear Data Tables 11, 569, (1973).
- LS78 C.M. Lederer and V.S. Shirley, Table of the Isotopes, 7th Edition, John Wiley & Sons, Inc., New York (1978)
- MDR88 V. McLane, C.L. Dunford and P.F. Rose, Neutron Cross Sections, Vol. 2 - Neutron Cross Section Curves, Academic Press, Inc., Boston (1988).
- MS80 J.W. Meadows and D.L. Smith, Report ANL/NDM-53, Argonne National Laboratory (1980).
- MSW80 J.W. Meadows, D.L. Smith and G. Winkler, Nuclear Instruments and Methods 176, 439 (1980).
- OT86 N. Olson and B. Trostell, Nucl. Instr. Meth. A245, 415 (1986).
- Qai91 Proceedings of the International Conference on Nuclear Data for Science and Technology, ed. S.M. Qaim, Juelich, Germany, 13-17 May 1991 (to be published).
- Ric60 A.C. Richardson, Rev. of Sci. Instr. 31, 11, 1202 (1960).
- SCW67 R.F. Seiler, M.R. Cleland and H.E. Wegner, Rev. of Sci. Instr. 38, 972 (1967).

- SM74 D.L. Smith and J.W. Meadows, Report ANL/NDM-9, Argonne National Laboratory (1974).
- SM86 D.L. Smith and J.W. Meadows, Report ANL/NDM-95, Argonne National Laboratory (1986).
- Tul90 J.K. Tuli, "Nuclear Wallet Cards", National Nuclear Data Center, Brookhaven National Laboratory, Upton, New York, 1973, U.S.A. (1990).
- Utt83 C.A. Uttley, "Sources of Monoenergetic Neutrons", Neutron Sources for Basic Physics and Applications, ed. S. Cierjacks, Pergamon Press, Oxford, U.K. (1983).
- Wea86 CRC Handbook of Chemistry and Physics, ed. R.C. Weast, CRC Press, Inc., Boca Raton, Florida (1986).
- Woj+88 P.W. Wojciechowski et al., J. Appl. Radiat. Isot. 39, 5, 429, (1988).

Table 1: List of elements that were examined in the process of designing the gas target

Element	Isotope	Abundance (%)*
Aluminum	Al-27	100
Carbon	C-12	98.9
	C-13	1.1
Chromium	Cr-50	4.35
	Cr-52	83.79
	Cr-53	9.5
	Cr-54	2.36
Cobalt	Co-59	100
Copper	Cu-63	69.17
	Cu-65	30.83
Fluorine	F-19	100
Gold	Au-197	100
Iron	Fe-54	5.9
	Fe-56	91.72
	Fe-57	2.1
	Fe-58	0.28
Molybdenum	Mo-92	14.84
	Mo-94	9.25
	Mo-95	15.92
	Mo-96	16.68
	Mo-97	9.55
	Mo-98	24.13
	Mo-100	9.63
Nickel	Ni-58	68.08
	Ni-60	26.22
	Ni-61	1.14
	Ni-62	3.63
Platinum	Pt-190	0.01
	Pt-192	0.79
	Pt-194	32.9
	Pt-195	33.8
	Pt-196	25.3
	Pt-198	7.2
Tantalum	Ta-181	100

Table 1: continued

Element	Isotope	Abundances (%)*
Titanium	Ti-46	8.0
	Ti-47	7.3
	Ti-48	73.8
	Ti-49	5.5
	Ti-50	5.4
Tungsten	W-180	0.12
	W-182	26.3
	W-183	14.28
	W-184	30.7
	W-186	28.6
Vanadium	V-50	0.25
	V-51	99.75

* J. K. Tuli [Tul90]. Note that due to round-off errors, the total for all stable isotopes of a particular element may not equal exactly 100%.

Table 2: Melting points and thermal conductivities for several materials considered in the target design

Material	Melting Point (°K)*	Thermal Conductivity (watts/cm/°K)*
Aluminum (Al)	933	2.37
Carbon (C)	3823	0.0159
Chromium (Cr)	2130	0.939
Cobalt (Co)	1768	1.00
Copper (Cu)	1356	4.01
Gold (Au)	1338	3.18
Iron (Fe)	1808	0.804
Molybdenum (Mo)	2890	1.38
Nickel (Ni)	1726	0.909
Platinum (Pt)	2045	0.716
Tantalum (Ta)	3269	0.575
Titanium (Ti)	1933	0.219
Tungsten (W)	3683	1.73
Vanadium (V)	2163	0.307

* R.C. Weast [Wea86]. Note that absolute zero on the Kelvin scale is equivalent to -273.15 degrees on the Centigrade scale. Thermal conductivity values correspond to 298.15 degrees Kelvin (25 degrees centigrade). These conductivity values do not vary dramatically with temperatures over the expected operating range of temperatures for the gas target.

Table 3: Features of (d,n) reactions for various materials which have been considered for the target beam stop, beam aperture and gas-cell window

Element	Isotope	Reaction Product#	Q-value (MeV)**	Threshold (MeV)*	Mean Life (τ)**	Decay Modes**
C	C-12	N-13	-0.28	0.33	14.38 m	ϵ
	C-13	N-14	5.327	--	stable	--
Ta	Ta-181	W-182	4.871	--	stable	--
W	W-180	Re-181	1.878	--	28.71 h	ϵ
	W-181	Re-183	2.628	--	101.0 h	ϵ
	W-183	Re-184	2.916	--	54.82 d	ϵ
	W-184	Re-185	3.182	--	stable	--
	W-186	Re-187	3.772	--	6.3×10^{10} y	β -
Au	Au-197	Hg-198	4.879	--	stable	--
Mo	Mo-92	Tc-93	1.863	--	3.97 h	ϵ
	Mo-94	Tc-95	2.670	--	28.85 h	ϵ
	Mo-95	Tc-96	3.175	--	6.17 d	ϵ
	Mo-96	Tc-97	3.495	--	3.74×10^6 y	ϵ
	Mo-97	Tc-98	3.952	--	6.05×10^6 y	β -
	Mo-98	Tc-99	4.276	--	3.04×10^5 y	β -
	Mo-100	Tc-101	5.216	--	20.45 m	β -

* There is no threshold energy when the Q-value is greater than or equal to zero.

** J.K. Tule [Tul90]. Note: s = seconds, m = minutes, h = hours, d = days, y = years.

Even though there may be isomer excitation in certain instances, only those products in the ground state are considered here, for convenience.

Table 4: Features of (d,p) reactions for various materials which have been considered for the target beam stop, beam aperture and gas-cell window

Element	Isotope	Reaction Product#	Q-value (MeV)**	Threshold (MeV)*	Mean Life (τ)**	Decay Modes**
C	C-12	C-13	2.722	--	stable	--
	C-13	C-14	5.952	--	8267.0 y	β^-
Ta	Ta-181	Ta-182	3.839	--	165.1 d	β^-
W	W-180	W-181	4.456	--	174.9 d	ϵ
	W-182	W-183	3.966	--	stable	--
	W-183	W-184	5.187	--	stable	--
	W-184	W-185	3.531	--	108.3 d	β^-
	W-186	W-187	3.242	--	34.2 h	β^-
Au	Au-197	Au-198	4.288	--	3.886 d	β^-
Mo	Mo-92	Mo-93	5.843	--	5.05 x 10 ³ y	ϵ
	Mo-94	Mo-95	5.143	--	stable	--
	Mo-95	Mo-96	6.930	--	stable	--
	Mo-96	Mo-97	4.597	--	stable	--
	Mo-97	Mo-98	6.418	--	stable	--
	Mo-98	Mo-99	3.701	--	95.1 h	β^-
	Mo-100	Mo-101	3.174	--	21 m	β^-

* There is a threshold energy when the Q-value than zero.

** J.K. Tule [Tul90]. Note: s = seconds, m = minutes, h = hours, d = days, y = years.

Even though there may be isomer excitations in certain instances, only those transitions leading to reaction products in the ground state are considered here, for convenience.

Table 5: Features of (n,d) reactions for various materials which have been considered for fabrication of the gas target

Elem.	Isot.†	React. Prod.®	Q-value (MeV)**	Thresh. (MeV)*	Cross Sect. #	Mean Life (τ)**	Decay Modes**
Al	Al-27	Mg-26	-6.048	6.274	<10	stable	--
Cu	Cu-63	Ni-62	-3.898	3.960	<3	stable	--
	Cu-65	Ni-64	-5.229	5.310	<2	stable	--
Fe	Fe-54	Mn-53	-6.629	6.753	<5	5.33 x 10 ⁶ y	ϵ
	Fe-56	Mn-55	-7.960	8.103	<3	stable	--
	Fe-57	Mn-56	-8.336	8.484	<2	3.72 h	β -
Co	Co-59	Fe-58	-5.140	5.228	<10	stable	--
Cr	Cr-50	V-49	-7.366	7.515	<10	488 d	ϵ
	Cr-52	V-51	-8.281	8.441	<5	stable	--
	Cr-53	V-52	-8.909	9.079	<5	5.41 m	β -
	Cr-54	V-53	-10.149	10.339	<3	2.32 m	β -
Ni	Ni-58	Co-57	-5.948	6.051	2.5	392.1 d	ϵ
	Ni-60	Co-59	-7.309	7.432	<2	stable	--
	Ni-61	Co-60	-7.638	7.764	<2	7.605 y	β -
	Ni-62	Co-61	-8.913	9.058	<1	2.38 h	β -
V	V-51	Ti-50	-5.838	5.953	<5	stable	--
F	F-19	O-18	-5.770	6.076	<20	stable	--
Ti	Ti-46	Sc-45	-8.121	8.299	<5	stable	--
	Ti-47	Sc-46	-8.238	8.415	<5	120.91 d	β -
	Ti-48	Sc-47	-9.222	9.416	<3	4.826 d	β -
	Ti-49	Sc-48	-9.131	9.319	<3	63.05 h	β -
	Ti-50	Sc-49	-9.941	10.14	<2	82.52 m	β -

* There is a threshold energy when the Q-value is less than zero.
 ** J.K. Tule [Tul90]. Note: s = seconds, m = minutes, h = hours, d = days, y = years.
 # McLane et al. [MDR88]. Cross sections in mb (millibarn) are for 10 MeV neutrons. Rough estimates based on systematics are provided when specific values were not available.
 † Isotopes with very small abundances are ignored in this table.
 ® Even though there may be isomer excitations in certain instances, only those transitions leading to reaction products in the ground state are considered here, for convenience.

Table 6: Features of (n,p) reactions for various materials which have been considered for fabrication of the gas target

Elem.	Isot.†	React. Prod.®	Q-value (MeV)**	Thresh. (MeV)*	Cross Sect. #	Mean Life (τ)**	Decay Modes**
Al	Al-27	Mg-27	-1.829	1.897	100	13.65 m	β^-
Cu	Cu-63	Ni-63	0.716	--	<200	144.4 y	β^-
	Cu-65	Ni-65	-1.356	1.377	12	3.63 h	β^-
Fe	Fe-54	Mn-54	0.085	--	470	450.3 d	ϵ, β^-
	Fe-56	Mn-56	-2.914	2.966	70	3.720 h	β^-
	Fe-57	Mn-57	-1.909	1.942	<50	125.8 s	β^-
Co	Co-59	Fe-59	-0.783	0.796	45	64.19 d	β^-
Cr	Cr-50	V-50	-0.256	0.261	<400	2.16×10^{17} y	ϵ, β^-
	Cr-52	V-52	-3.194	3.256	80	5.41 m	β^-
	Cr-53	V-53	-2.654	2.704	25	2.32 m	β^-
	Cr-54	V-54	-6.259	6.376	<10	71.85 s	β^-
Ni	Ni-58	Co-58	0.401	--	600	102.2 d	ϵ
	Ni-60	Co-60	-2.042	2.076	185	7.605 y	β^-
	Ni-61	Co-61	-0.540	0.549	85	2.38 h	β^-
	Ni-62	Co-62	-4.459	4.531	<10	2.16 m	β^-
V	V-51	Ti-51	-1.691	1.724	20	8.31 m	β^-
F	F-19	O-19	-4.037	4.250	35	38.82 s	β^-
Ti	Ti-46	Sc-46	-1.585	1.620	250	120.91 d	β^-
	Ti-47	Sc-47	0.181	--	90	4.826 d	β^-
	Ti-48	Sc-48	-3.213	3.280	30	63.05 h	β^-
	Ti-49	Sc-49	-1.218	1.243	<30	82.52 m	β^-
	Ti-50	Sc-50	-6.107	6.230	<10	147.9 s	β^-

* There is no threshold energy when the Q-value is greater than or equal to zero.

** J.K. Tule [Tul90]. Note: s = seconds, m = minutes, h = hours, d = days, y = years.

McLane et al. [MDR88]. Cross sections in mb (millibarn) are for 10 MeV neutrons. Rough estimates based on systematics are provided when specific values were not available.

† Isotopes with very small abundances are ignored in this table.

® Even though these may be isomer excitations in certain instances, only those transitions leading to reaction products in the ground state are considered here, for convenience.

Table 7: Features of (n,a) reactions for various materials which have been considered for fabrication of the gas target

Elem.	Isot.†	React. Prod.©	Q-value (MeV)**	Thresh. (MeV)*	Cross Sect.#	Mean Life (τ)**	Decay Modes**
Al	Al-27	Na-24	-3.130	3.246	90	21.58 h	β^-
Cu	Cu-63	Co-60	1.715	--	50	7.605 y	β^-
	Cu-65	Co-62	-0.111	0.195	<2	2.16 m	β^-
Fe	Fe-54	Cr-51	0.844	--	65	39.97 d	ϵ
	Fe-56	Cr-53	0.326	--	<20	stable	--
	Fe-57	Cr-54	2.399	--	<30	stable	--
Co	Co-59	Mn-56	0.328	--	17	3.71 h	β^-
Cr	Cr-50	Ti-47	0.321	--	<50	stable	--
	Cr-52	Ti-49	-1.209	1.232	<30	stable	--
	Cr-53	Ti-50	1.791	--	<50	stable	--
	Cr-54	Ti-51	-1.557	1.586	<10	8.31 m	β^-
Ni	Ni-58	Fe-55	2.898	--	127	3.93 y	ϵ
	Ni-60	Fe-57	1.355	--	<50	stable	--
	Ni-61	Fe-58	3.579	--	<50	stable	--
	Ni-62	Fe-59	-0.437	0.444	<20	64.19 d	β^-
V	V-51	Sc-48	-2.060	2.101	5	63.05 h	β^-
F	F-19	N-16	-1.522	1.603	60	10.27 s	β^- , β^- a
Ti	Ti-46	Ca-43	-0.071	0.073	<50	stable	--
	Ti-47	Ca-44	2.185	--	<50	stable	--
	Ti-48	Ca-45	-2.028	2.071	<20	236.3 d	β^-
	Ti-49	Ca-46	0.229	--	<50	stable	--
	Ti-50	Ca-47	-3.434	3.503	<10	6.53 d	β^-

* There is no threshold energy when the Q-value is greater than or equal to zero.

** J.K. Tule [Tul90]. Note: s = seconds, m = minutes, h = hours, d = days, y = years.

McLane et al. [MDR88]. Cross sections in mb (millibarn) are for 10 MeV neutrons. Rough estimates based on systematics are provided when specific values were not available.

† Isotopes with very small abundances are ignored in this table.

© Even though there may be isomer excitations in certain instances, only those transitions leading to reaction products in the ground state are considered here for convenience.

Table 8: Features of (n,2n) and (n,np) reactions for various materials which have been considered for fabrication of the gas target##

Reaction	Q-value (MeV)**	Thresh. (MeV)*	Cross Sect. #	Mean Life (τ)**	Decay Modes**
Fe-57(n,2n)Fe-56	-7.646	7.781	<100	stable	--
Cr-53(n,2n)Cr-52	-7.939	8.090	<100	stable	--
Cr-54(n,2n)Cr-53	-9.719	9.901	<50	stable	--
Fe-54(n,np)Mn-53	-8.853	9.018	<50	5.33 x 10 ⁶ y	ϵ
Co-59(n,np)Fe-58	-7.364	7.490	<10	stable	--
Cr-50(n,np)V-49	-9.590	9.784	<1	488.0 d	ϵ
Ni-58(n,np)Co-57	-8.172	8.314	<50	392.1 d	ϵ
Ni-60(n,np)Co-59	-9.533	9.694	<5	stable	--
Cu-63(n,np)Ni-62	-6.122	6.220	<100	stable	--
Cu-65(n,np)Ni-64	-7.453	7.569	<10	stable	--
Al-27(n,np)Mg-26	-8.272	8.581	<10	stable	--
V-51(n,np)Ti-50	-8.062	8.222	<10	stable	--
F-19(n,np)O-18	-7.994	8.418	<10	stable	--

- * There is a threshold energy when the Q-value is less than zero.
 ** J.K. Tule [Tul90]. Note: s = seconds, m = minutes, h = hours, d = days, y = years.
 # McLane et al. [MDR88]. Cross sections in mb (millibarn) are for 10 MeV neutrons. Rough estimates based on systematics are provided when specific values were not available.
 ## Only those processes with neutron-energy thresholds below 10 MeV are included.

Table 9: Calculated relative radiation vulnerability parameters (VA) for aluminum and copper*

Reaction	VA(1 h)	VA(1 d)	VA(1 w)	VA(1 m)	VA(1 y)
Al-27(n,p)Mg-27	129.1	0	0	0	0
Al-27(n, α)Na-24	96.5	33.3	0.046	0	0
Al-27(n,d+np)Mg-26	0	0	0	0	0
Total (Al)	225.6	33.3	0.046	0	0
Cu-63(n,p)Ni-63	0.0026	0.0026	0.0026	0.0026	< 0.0026
Cu-63(n, α)Co-60	0.012	0.012	0.012	0.012	< 0.012
Cu-63(n,d+np)Ni-62	0	0	0	0	0
Cu-65(n,p)Ni-65	18.7	0.033	0	0	0
Cu-65(n, α)Co-62	0	0	0	0	0
Cu-65(n,d)Ni-64	0	0	0	0	0
Total (Cu)	18.71	0.0476	0.0146	0.0146	< 0.0146

* Note: h = hour; d = day; w = week; m = month; y = year.

Table 10: Calculated relative radiation-vulnerability parameters (VA) for gold, tantalum, tungsten, carbon and molybdenum*

Reaction	VA(1 h)	VA(1 d)	VA(1 w)	VA(1 m)	VA(1 y)
Au- 197(d,n)Hg- 198	0	0	0	0	0
Au- 197(d,p)Au- 198	<u>0.25</u>	<u>0.2</u>	<u>0.042</u>	<u>0.00012</u>	<u>0</u>
Total (Au)	0.25	0.2	0.042	0.00012	0
Ta- 181(d,n)W- 182	0	0	0	0	0
Ta- 181(d,p)Ta- 182	<u>0.0061</u>	<u>0.006</u>	<u>0.0058</u>	<u>0.005</u>	<u>0.00066</u>
Total (Ta)	0.0061	0.006	0.0058	0.005	0.00066
W- 182(d,n)Re- 183	0.062	0.049	0.012	0.000050	0
W- 182(d,p)W- 183	0	0	0	0	0
W- 183(d,n)Re- 184	0.0026	0.0026	0.0023	0.0015	0.0000033
W- 183(d,p)W- 184	0	0	0	0	0
W- 184(d,n)Re- 185	0	0	0	0	0
W- 184(d,p)W- 185	0.0028	0.0028	0.00266	0.00215	0.000098
W- 186(d,n)Re- 187	0	0	0	0	0
W- 186(d,p)W- 187	<u>0.195</u>	<u>0.099</u>	<u>0.00148</u>	<u>0</u>	<u>0</u>
Total (W)	0.2624	0.1534	0.01844	0.0037	0.000101
C- 12(d,n)N- 13	1.527	0	0	0	0
C- 12(d,p)C- 13	0	0	0	0	0
C- 13(d,n)N- 14	0	0	0	0	0
C- 13(d,p)C- 14	<u>3.7x10⁻⁹</u>	<u>3.7x10⁻⁹</u>	<u>3.7x10⁻⁹</u>	<u>3.7x10⁻⁹</u>	<u>3.7x10⁻⁹</u>
Total (C)	1.527	3.7x10 ⁻⁹	3.7x10 ⁻⁹	3.7x10 ⁻⁹	3.7x10 ⁻⁹

Table 10: continued

Reaction	VA(1 h)	VA(1 d)	VA(1 w)	VA(1 m)	VA(1 y)
Mo-92(d,n)Tc-93	0.697	0.0021	0	0	0
Mo-92(d,p)Mo-93	8.06×10^{-8}				
Mo-94(d,n)Tc-95	0.0744	0.0335	2.28×10^{-4}	0	0
Mo-94(d,p)Mo-95	0	0	0	0	0
Mo-95(d,n)Tc-96	0.0257	0.022	0.00829	2.0×10^{-4}	0
Mo-95(d,p)Mo-96	0	0	0	0	0
Mo-96(d,n)Tc-97	1.24×10^{-10}				
Mo-96(d,p)Mo-97	0	0	0	0	0
Mo-97(d,n)Tc-98	4.3×10^{-11}				
Mo-97(d,p)Mo-98	0	0	0	0	0
Mo-98(d,n)Tc-99	2.17×10^{-9}				
Mo-98(d,p)Mo-99	6.03×10^{-2}	4.73×10^{-2}	0.0104	3.14×10^{-5}	0
Mo-100(d,n)Tc-101	0.36	0	0	0	0
Mo-100(d,p)Mo-101	0.38	0	0	0	0
Total (Mo)	1.597	0.1049	0.0189	2.31×10^{-4}	8.29×10^{-8}

* Only major isotopes are considered for these elements.

Table 11: Macroscopic elastic scattering cross sections for various materials which have been considered for fabrication of the gas target

Element**	Elastic Scat. Cross Section# (b)	Density (g/cm ³)	Atomic Weight (amu)	Macroscopic Cross Section* (cm ⁻¹)
C	0.6	1.95	12.011	0.0587
Al	0.7	2.6989	26.9815	0.0422
Ti	1.5	4.54	47.88	0.0857
V	1.95	6.11	50.9415	0.1409
Cr	1.55	7.19	51.9961	0.1291
Fe	1.6	7.874	55.847	0.1359
Co	2.0	8.9	58.9332	0.1819
Ni	1.85	8.902	58.69	0.1690
Cu	1.8	8.96	63.546	0.1529
Mo	2.5	10.22	95.94	0.1604
Ta	2.6	16.654	180.9479	0.1441
W	2.5	19.3	183.85	0.1581
Au	2.4	19.3	196.9665	0.1417
Nylon†	0.6†	1.29†	12.011†	0.3881†

** Or a neighboring element for which the elastic scattering cross-section at 10 MeV is known. Integrated elastic scattering cross sections vary slowly with atomic number.

† The density of nylon is 1.4 g/cm³. It is assumed that nylon is a polymer with roughly equal parts of hydrogen and carbon, therefore the density of carbon is 1.29 g/cm³ in nylon. It is the carbon content of nylon which is considered for scattering purposes in the present analysis, because hydrogen does not scatter toward back angles.

Angle-integrated cross section from McLane et al. [MDR88].
* Equivalent to the scattering vulnerability parameter, Vs, as given by Eq. (2).

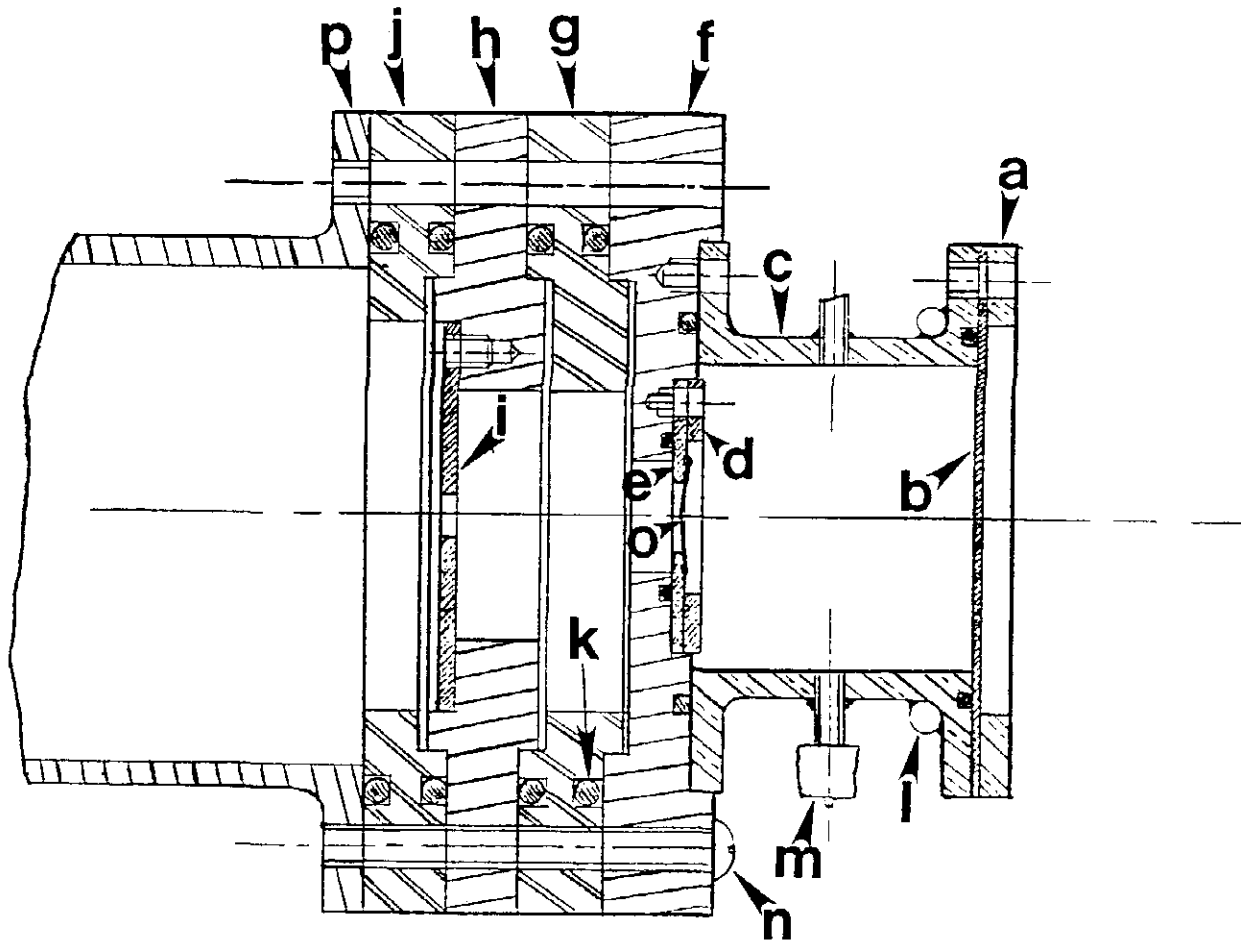


Figure 1: Cutaway schematic side view of the target assembly. The individual components are identified as follows: a) beam-stop ring, b) beam stop, c) gas cell d) foil-support ring, e) foil support, f) foil-aperture flange, g) front-isolation flange, h) aperture flange, i) aperture plate, j) back-isolation flange, k) U-ring(s) l) water-cooling tubing, m) gas tubing, n) insulated assembly screw(s), and o) molybdenum-window foil.

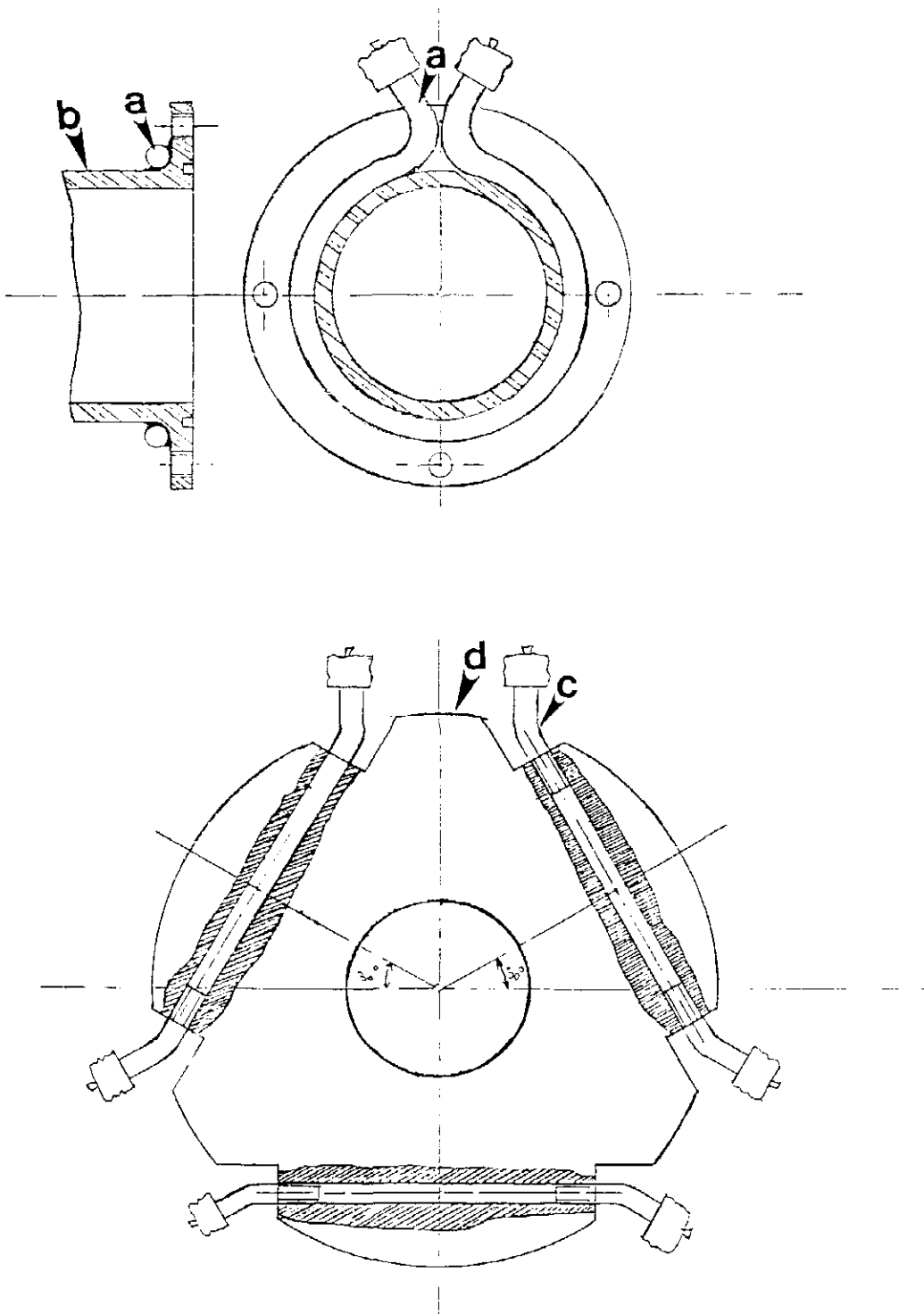
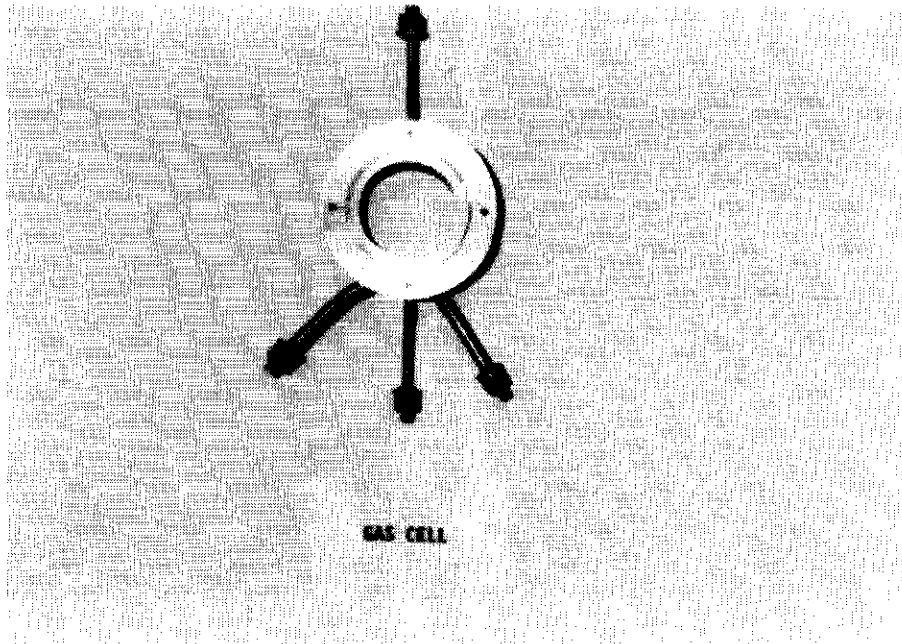


Figure 2: Cutaway schematic views of the critical cooling tubing and channels of the target assembly. The components identified are as follows: a) gas-cell cooling tubing, b) gas-cell body, c) cooling tubing and channels in the aperture flange and foil-aperture flange. d) aperture flange or foil-aperture flange (both have identical cooling channels).

A



B

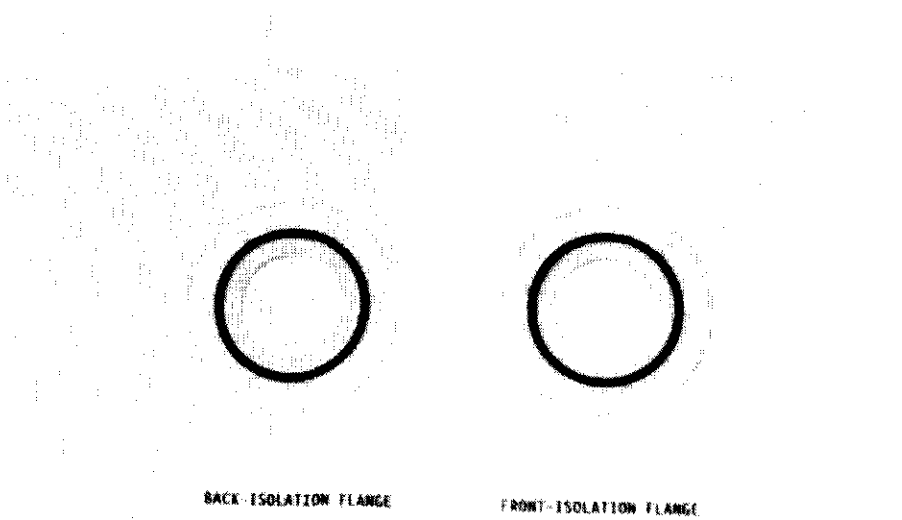
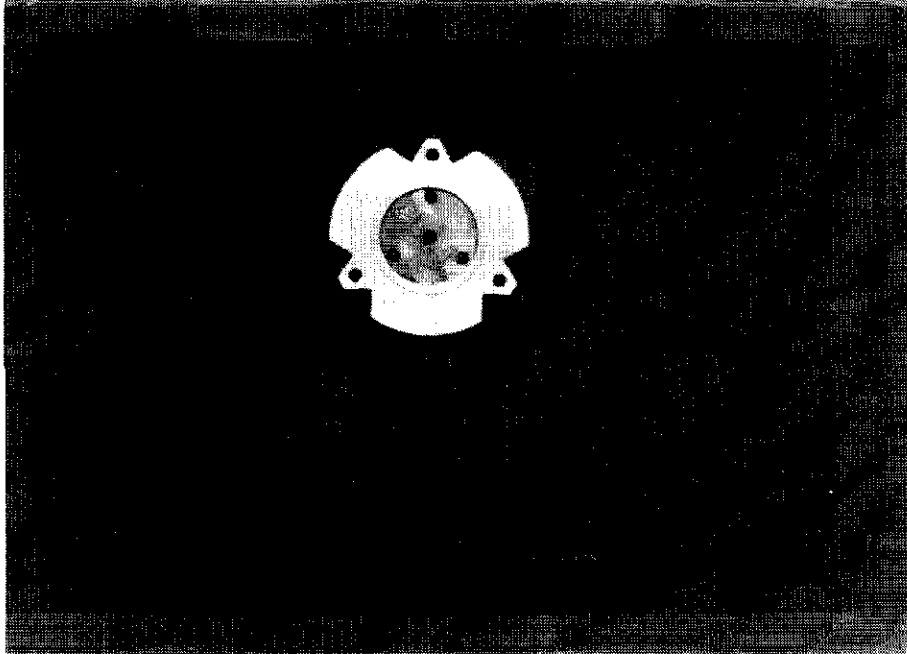


Figure 3: Photographs of selected components of the gas-target assembly. shown are: a) an end view of the gas cell, and b) the front-isolation flange and back-isolation flange.

A



B

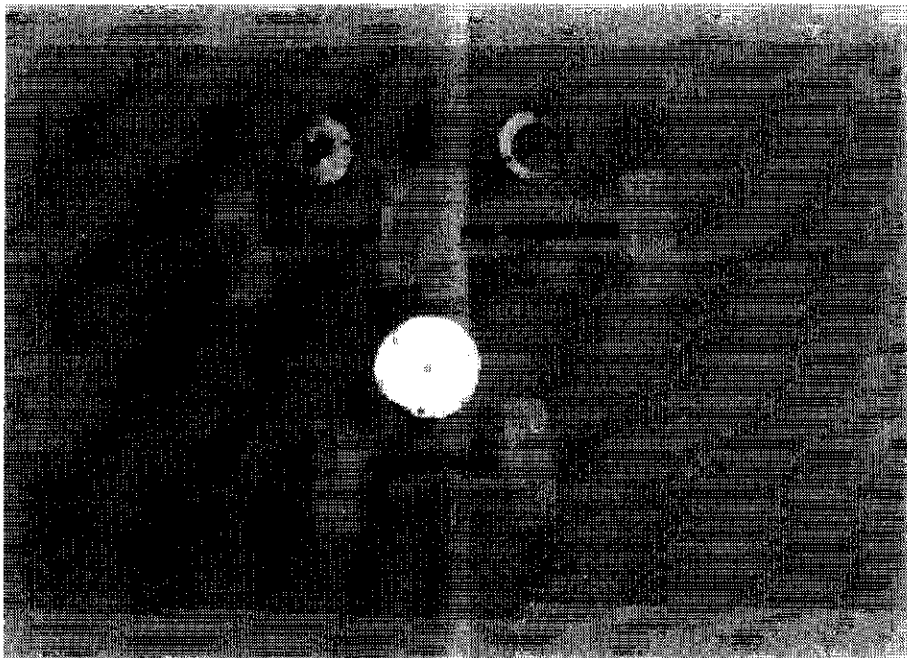
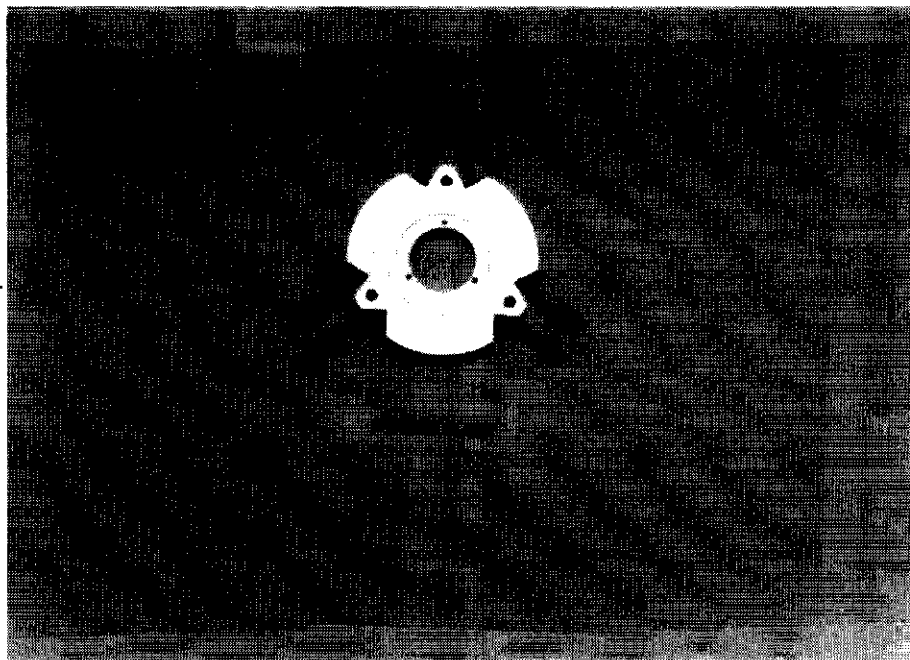


Figure 4: Photographs of selected components of the gas-target assembly. Shown are: a) the assembled aperture flange and aperture plate, and b) the foil support, the foil-support ring, and the aperture plate.

A



B

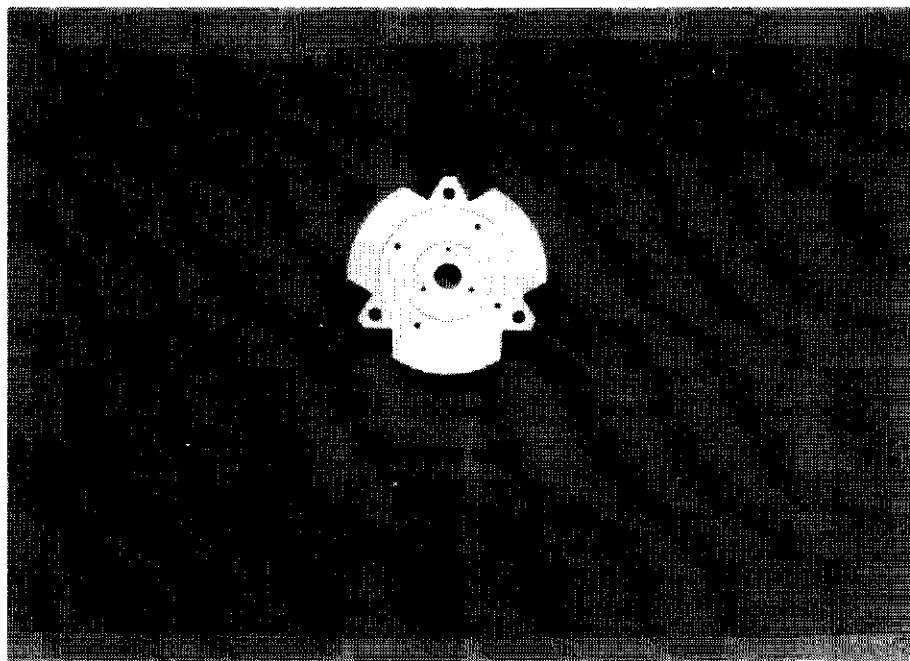
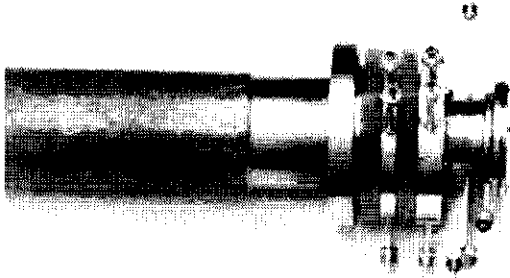


Figure 5: Photographs of selected components of the gas-target assembly. Shown are: a) the aperture flange, and b) the foil-aperture flange.

A



B

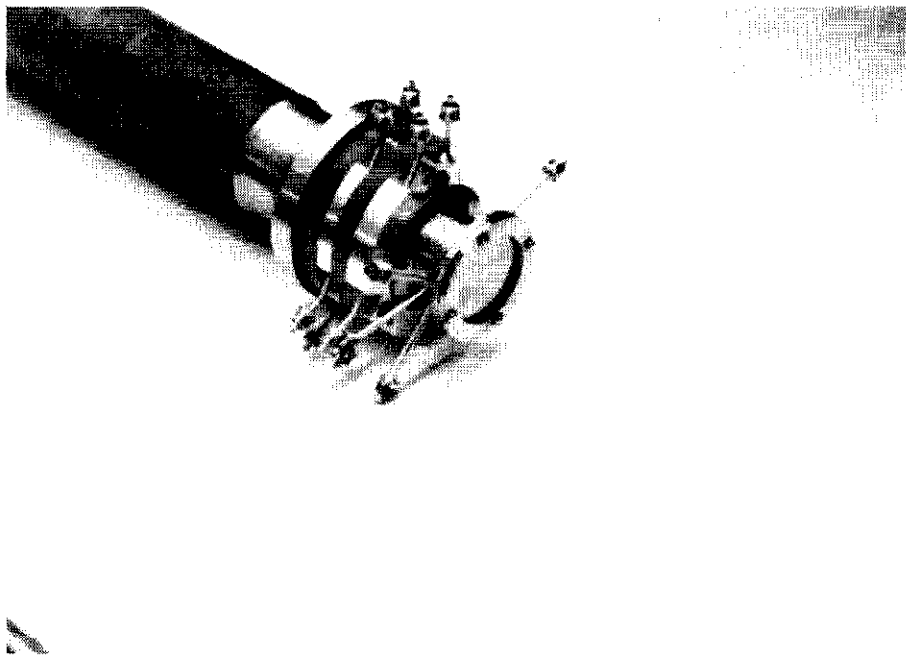
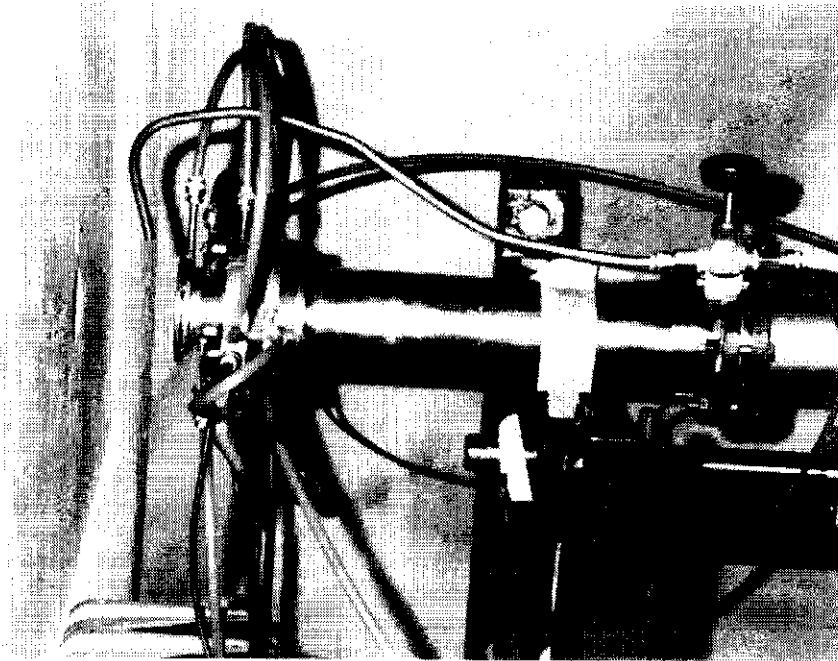


Figure 6: Assembly views of the gas target. Shown are: a) full-side view, and b) oblique view.

A



B

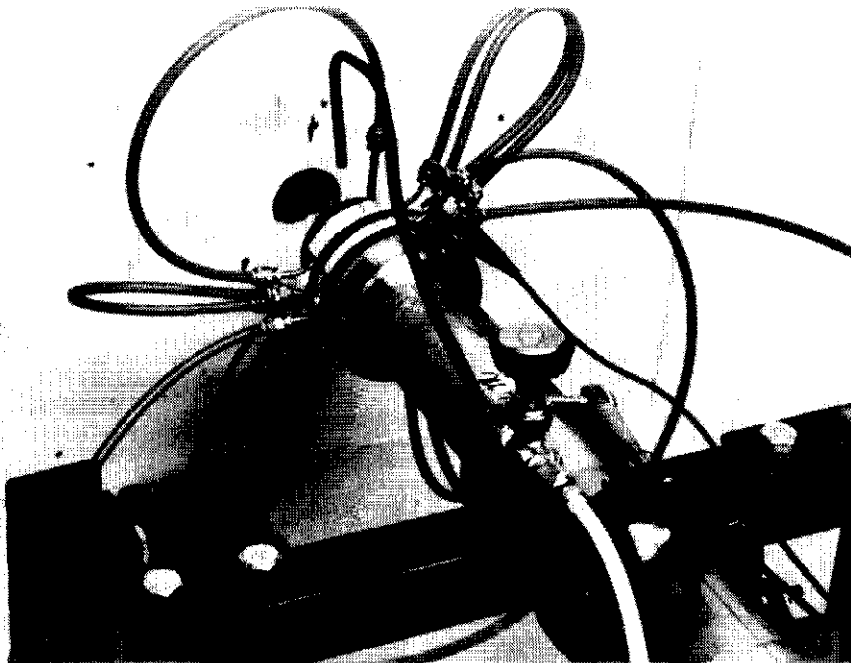


Figure 7: Views of the gas target fully assembled on a beam line of the accelerator (including all attached water-cooling and deuterium-gas lines). shown are: a) full-side view, and b) oblique view from a back angle.